ELSEVIER

Journal of Chromatography A, 877 (2000) 1–11

JOURNAL OF CHROMATOGRAPHY A

www.elsevier.com/locate/chroma

Adsorption equilibria and overloaded band profiles of basic drugs in a reversed-phase system

Igor Quiñones[a,b], Alberto Cavazzini[a,b,1], Georges Guiochon[a,b,*]

[a]*Department of Chemistry and Department of Chemical Engineering, University of Tennessee, Knoxville, TN 37996-1600, USA*
[b]*Division of Chemical and Analytical Sciences, Oak Ridge National Laboratory, Oak Ridge, TN 37831-6120, USA*

Received 21 October 1999; received in revised form 7 February 2000; accepted 8 February 2000

Abstract

Single-solute adsorption equilibrium isotherms of three basic drugs: buspirone, doxepin and diltiazem were determined by frontal analysis in a reversed-phase system composed of an octadecylsilica packing material and a buffered mobile phase containing acetonitrile. The adsorption data were fitted to the bi-Langmuir model. Within the framework of this model, the adsorption of the drugs is assumed to occur on two distinct kinds of sites with different average adsorption energies. The data are consistent with the assumption that the low energy sites account for the hydrophobic interactions between the solutes and the chemically bonded alkyl chains and the high energy sites account for the ion-exchange interactions between the residual active silanols and the protonated bases. Multisolute, overloaded band profiles were also measured for the three binaries and for mixtures of the three drugs. Theoretical band profiles were calculated using the equilibrium dispersive model and the ideal adsorbed solution theory model which uses the parameters determined from the correlation of the single-solute adsorption data. Good agreement was found between the experimental and calculated overloaded band profiles.

Keywords: Adsorption isotherms; Band profiles; Mathematical modeling; Buspirone; Doxepin; Diltiazem

1. Introduction

High-efficiency adsorption-based separation processes like batch elution chromatography and simulated moving bed chromatography have became important purification techniques, widely used in the pharmaceutical industry [1]. The scale-up and optimization of these processes requires accurate calculations of the overloaded, multisolute band profiles produced as a result of the separation. In order to perform such calculations, an accurate description of the associated adsorption equilibria is mandatory [2]. The validity of the procedure is now established [2]. Still, its application raises particular issues in difficult cases, such as the separation of basic compounds. The required equilibrium data are more difficult to measure than for the simpler systems preferred in fundamental studies, so difficult compromises are required.

The chromatography of amine bases is extremely

*Corresponding author. Department of Chemistry and Department of Chemical Engineering, University of Tennessee, Knoxville, TN 37996-1600, USA. Tel.: +1-865-9740-733; fax: +1-865-9742-667.

E-mail address: guiochon@utk.edu (G. Guiochon)

[1]Present address: Department of Chemistry, University of Ferrara, Via Luigi Borsari 46, I-44100 Ferrara, Italy.

0021-9673/00/$ – see front matter
PII: S0021-9673(00)00183-7

important since a vast majority of the known drugs are basic compounds. Unfortunately, there are many controversial opinions in the literature regarding the retention behavior of basic solutes, especially in reversed-phase chromatography [3]. This behavior is complex because different retention mechanisms are believed to contribute to the overall outcome of the separations. Among these mechanisms it is believed that the most important are: (i) hydrophobic interactions; (ii) ion-exchange; (iii) salting-out effects and (iv) hydrogen-bond interactions. As a result of the complexity of the interferences between these mechanisms, several phenomena are commonly observed when performing separations of basic compounds: (i) severe peak tailing; (ii) irreversible adsorption and (iii) low efficiency [3]. Unfortunately, it is not possible to identify mixed mechanisms using linear chromatography data. Only the modeling of isotherm data allow the separation and a proper estimate of the retention contributions of two mechanisms [4,5]. However, published adsorption data regarding basic compounds are scarce [6].

The essential goal of this paper was to illustrate how it is possible to determine the experimental data required for the prediction of multicomponent band profiles when dealing with mixtures of compounds the separation of which raises difficult practical problems. We selected for this purpose a small group of basic drugs as the solutes, a C_{18} silica column eluted with a mixture of acetonitrile and a phosphate buffer as the phase system, and the prediction of overloaded multicomponent bands and system peaks as the validation method. Equilibrium data for only the single components could be acquired during the time allotted to the study. These data were acquired by frontal analysis and interpreted using a suitable isotherm model. A multicomponent, competitive model was constructed from these single-component isotherms. Band profiles were calculated via the equilibrium–dispersive model, with the same conditions under which experimental overloaded band profiles were obtained for different mixtures of these compounds. The comparison between experimental and calculated profiles constitutes an indirect but sensitive test of the ability to predict correctly competitive adsorption data based on the parameters identified from the correlation of single-solute data.

2. Experimental

2.1. Equipment

The analytical chromatograms, overloaded band profiles and breakthrough curves used in frontal analysis (FA) were acquired using a HP 1100 series modular liquid chromatograph (Hewlett-Packard, Palo Alto, CA, USA). This instrument is composed of an isocratic pump, a vacuum degasser for the mobile phase, a variable-wavelength spectrophotometric detector, and a temperature-controlled column compartment. A personal computer-based software was used to control these modules and to acquire and process the UV signal. The system was complemented by a Rheodyne 7725i injector (Cotati, CA, USA) and a Gilson (Middletown, WI, USA) Model 203 fraction collector.

The single-component overloaded band profiles were measured via fraction collection. The collected fractions were further analyzed using an HP 1090 series liquid chromatograph (Hewlett-Packard) equipped with a ternary solvent delivery system, an automatic sample injector with a 25-μl loop, a diode-array UV detector, and a personal computer-based data acquisition/processing system.

2.2. Materials

A 150 mm×3.9 mm I.D. YMC-Basic C_{18} column (YMC, Wilmington, NC, USA) was used to measure the adsorption data. The particle size was 5 μm, the average pore size was 120 Å and the void fraction of the column was $\epsilon_T=0.76$. Using a mixture of the three solutes, this column was characterized periodically by elution chromatography. The efficiency and retention data were found to remain essentially unchanged during the entire study. This column belongs to the so called ''base-deactivated'' columns, usually employed in the separation of basic compounds.

In all the experiments the mobile phase was a mixture of acetonitrile (ACN)–aqueous buffer (35:65, v/v). The buffer was prepared by mixing 0.1 *M* aqueous solutions of H_3PO_4 (analytical reagent, Mallinckrodt, Paris, KY, USA) and KH_2PO_4 (99.5+ %, Fluka, Ronkonkoma, NY, USA) until pH 3.0 was

reached. Acetonitrile and water were HPLC-grade, purchased from Fisher Scientific (Pittsburgh, PA, USA).

The solutes used in this work were three drugs [7]: the anxiolytic buspirone hydrochloride (8-{4-[4-(2-pyrimidinyl)-1-piperazinyl]butyl}-8-azaspiro[4,5]-decane-7,9-dione), $C_2H_2N_5O_2$, HCl (99% by thin-layer chromatography, TLC, Sigma, St. Louis, MO, USA); the antidepressant doxepin hydrochloride {11-(3-dimethylamino) - propylidene - 6, 11 - dihydrodibenz - [*b*,*e*]oxepine}, $C_{19}H_2NO$, HCl (98% by TLC, Sigma) and the Ca^{2+} blocker diltiazem hydrochloride {[2*S*-*cis*]-3-(acetyloxy)-5-[2-(dimethylamino)ethyl] - 2, 3 - dihydro - 2 - (4 - methoxyphenyl)-1,5-benzothiazepin-4(5H)-one}, $C_{22}H_{26}N_2O_4S$, HCl (99% by high-performance liquid chromatography, HPLC, Sigma). These are basic drugs whose structures are depicted in Fig. 1.

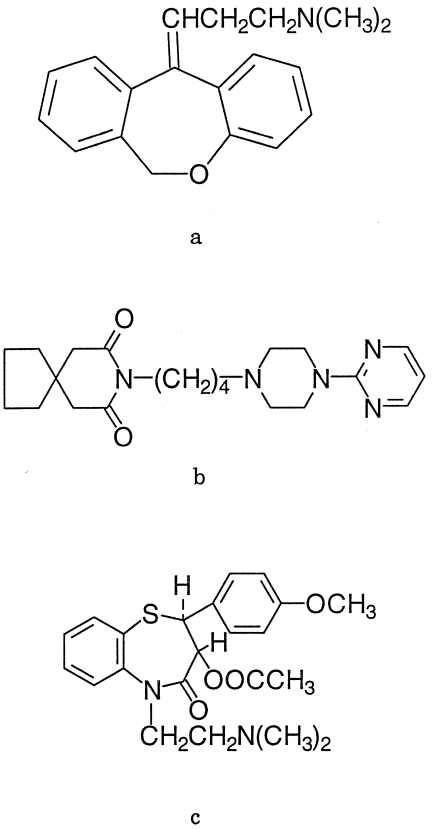

Fig. 1. Structures of (a) doxepin, (b) buspirone and (c) diltiazem.

A similar column was used to analyze the collected fractions. The buffer employed for quantitation was also 0.1 *M* phosphate but adjusted to pH 6.0 by mixing solutions of KH_2PO_4 (99.5+%, Fluka) and K_2HPO_4 (99.0+%, Fluka). We will use the indices 1, 2 and 3 when referring to buspirone (BU), doxepin (DO) and diltiazem (DI), respectively.

2.3. Procedures

The separation of the three compounds under analytical, i.e., linear conditions, at pH 3.0 and pH 6.0 is presented in Figs. 2 and 3, respectively. The parameters of these separations can be found in Table 1.

The adsorption data were measured by frontal analysis, by pumping solutions of the drugs in the mobile phase. The solutions were prepared and used on the same day. The flow-rate was kept at 1 ml/min. The UV signal was recorded at 345 nm, 325 nm and 300 nm for BU, DO and DI, respectively. After a breakthrough curve was recorded, the solution was replaced with one of higher concentration. It was observed than a reequilibration time of 90 min was needed between successive injections in order to obtain reproducible results. Accordingly, only one

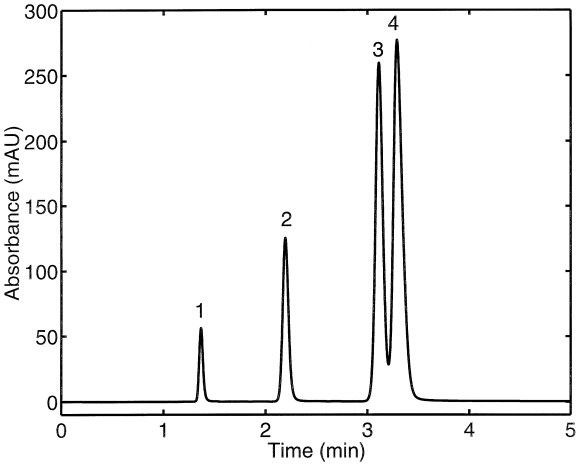

Fig. 2. Analytical separation of (1) thiourea, (2) buspirone, (3) diltiazem and (4) doxepin. Mobile phase is ACN–buffer (35:65); buffer is 0.1 *M* phosphate, pH 3.0, $T=25$ °C, flow-rate is 1 ml/min, injected volume is 20 μl with a concentration of 0.1 g/l, UV detection at 254 nm.

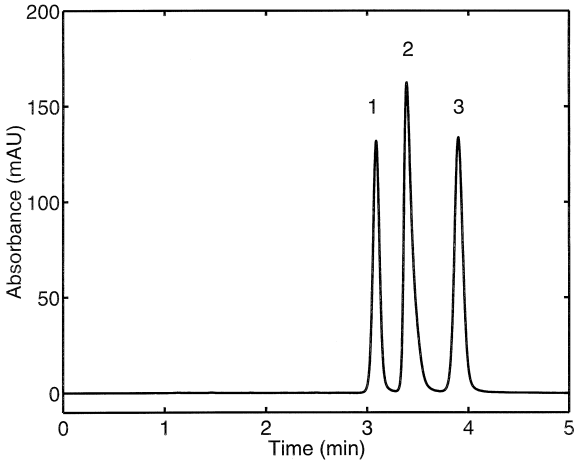

Fig. 3. Analytical separation of (1) buspirone, (2) doxepin and (3) diltiazem. Mobile phase is ACN–buffer (35:65); buffer is 0.1 *M* phosphate, pH 6.0, $T=25°C$, flow-rate is 1 ml/min, injected volume is 20 μl with a concentration of 0.1 g/l, UV detection at 254 nm.

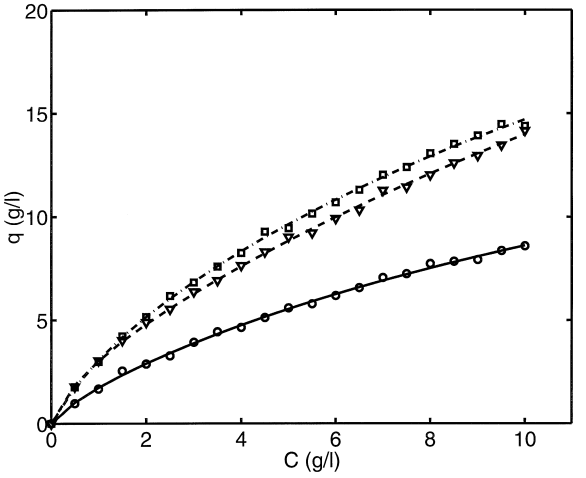

Fig. 4. Adsorption data of buspirone (circles), doxepin (triangles) and diltiazem (squares). Mobile phase is ACN–buffer (35:65); buffer is 0.1 *M* phosphate, pH 3.0, $T=25°C$.

adsorption data point per composition was measured in the systematic data acquisition campaigns. No multisolute adsorption data are reported.

Reported expressions [8] were used in order to calculate the adsorbed amounts from the FA breakthrough curves. Adsorption data determined via FA for the different solutes at 25°C are presented in Fig. 4 (symbols). In this figure the concentration in the mobile phase is represented by C and the concentration in the stationary phase by q.

The adsorption experiments carried out at low pH were made with rather concentrated solutions of phosphate buffers. Under these conditions, the stability of the C_{18} columns is limited since the buffers dissolve the silica [3]. So, after each experimental session, the columns were flushed first with several column volumes of a mixture of acetonitrile–pure water (1:1, v/v) and then they were flushed with pure acetonitrile.

The overloaded band profiles were acquired at 25°C. The single-solute band profiles were directly derived from the detector trace, converted to units of concentrations using a calibration polynomial. This polynomial was derived from the correlation of the UV-absorption signal associated with the FA plateaus and the corresponding total solute concentrations in the FA feed. The nonlinear detector response was converted using a third-order polynomial. Multisolute band profiles were obtained by collecting and analyzing successive fractions of the column effluent. Fractions were collected every 3 s (ca. 50 μl). They were then diluted prior to analysis. For quantitation, a linear calibration graph based on the area of the peak was established for each compound, via the external standard method. The analysis of the samples was performed at 27°C. The injected amount was 2 μl. The flow-rate was 1 ml/min. The signal was detected at 254 nm.

Table 1
Parameters of the separation under linear conditions

Parameter	Buspirone	Diltiazem	Doxepin
pH 3.0			
k'	0.606	1.281	1.411
N	7100	8500	6500
pH 6.0			
k'	1.256	1.846	1.522
N	8800	9100	7700

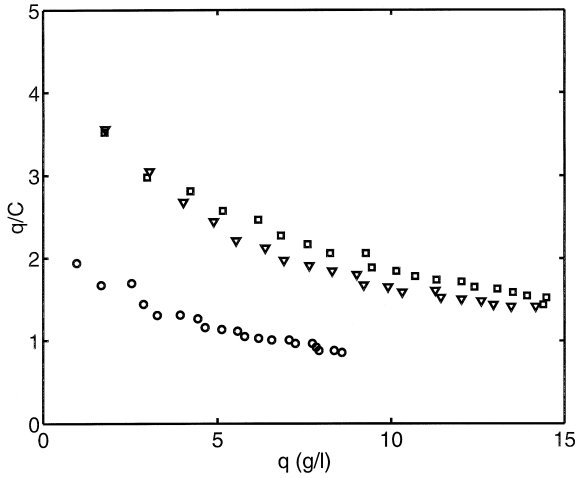

Fig. 5. Scatchard plot of the adsorption data of buspirone (circles), doxepin (triangles) and diltiazem (squares). Mobile phase is ACN–buffer (35:65); buffer is 0.1 *M* phosphate, pH 3.0, $T=25$°C.

3. Results

3.1. Adsorption equilibrium

Adsorption data were initially plotted in the form of a Scatchard plot, Fig. 5. Since the trend of the experimental data is clearly not linear, the Langmuir model is not likely to provide an adequate fit of the experimental results. Accordingly, we used the bi-Langmuir model to correlate the single-solute data under consideration. The model for the *i*th solute is defined as [2]:

$$q_{i,o} = f(C_{i,o}) = \frac{\Phi\kappa C_{i,o}}{1+\kappa C_{i,o}} + \frac{\Psi\lambda C_{i,o}}{1+\lambda C_{i,o}} \quad (1)$$

where Φ and Ψ are the saturation capacities of the two types of sites and κ and λ are the Langmuir equilibrium constants of the two types of sites, with $\Phi\kappa$ and $\Psi\lambda$ the corresponding Henry constant contributions. The subscript ''o'' emphasizes the fact that the correlation refers only to the single-solute adsorption data. Regression of the experimental adsorption data to the bi-Langmuir isotherm model was performed using a corrected Gauss–Newton method. The algorithm is implemented in the NAG Library [9]. The procedure calculates the values of the isotherm parameters which minimize the residual sum of squares between experimental and calculated values for each set of adsorption data. The parameters of the model are reported in Table 2 for each solute. As shown in Fig. 4 (lines), the model provides an excellent correlation of the experimental adsorption data (symbols).

Competitive adsorption data were predicted from the correlation of the single-solute data via the ideal adsorbed solution (IAS) model [10]. No assumptions have to be made regarding the nature of these data and any model could be used for the correlation provided that a good fit is obtained, especially at low concentrations.

The IAS model, derived within the framework of solution thermodynamics, assumes ideal behavior of both phases at equilibrium, viz. the adsorbed phase and the bulk fluid phase. Originally developed for gas adsorption, this model was later extended to adsorption from dilute liquid systems [11]. Within the scope of the model, a solvent-free mole fraction of the *i*th solute in the multicomponent adsorbed phase (x_i) is defined as:

$$x_i = \frac{q_i}{\sum_{i=1}^{N_s} q_i} \quad (2)$$

where N_s is the number of solutes in the system.

Table 2
Parameters of the bi-Langmuir model

Compound	Φ (g/l)	κ (l/g)	H	Ψ (g/l)	$\lambda\cdot10^2$(l/g)	Ψ/Φ
Buspirone	1.17	1.24	1.45	22.19	5.13	18.97
Doxepin	2.62	1.49	3.9	49.35	3.04	18.84
Diltiazem	3.31	0.74	2.45	36.45	4.78	11.01

The IAS model is defined by the following set of equations which are solved simultaneously in order to calculate all the values of the mole fractions x_i and the corresponding proportionality factors C_i°:

$$C_i = C_i^{\circ} x_i \tag{3a}$$

$$\Phi_1^{\circ} = \Phi_2^{\circ} = ... = \Phi_i^{\circ} = ... = \Phi_{N_s}^{\circ} \tag{3b}$$

$$\sum_{i=1}^{N_s} x_i = 1 \tag{3c}$$

In Eq. (3b) the integral for the spreading pressure of the single ith solute (Φ_i°) is defined by:

$$\Phi_i^{\circ} = \frac{\pi A}{RT} = \int_0^{C_i^{\circ}} \frac{f(C_{i,\mathrm{o}})}{C_{i,\mathrm{o}}} \mathrm{d}C_{i,\mathrm{o}} \tag{4}$$

where π is the spreading pressure, A is the specific surface area of the adsorbent, R is the gas constant and T is the absolute temperature.

Finally, the adsorbed amount of each solute in the multicomponent adsorbed phase is given by:

$$q_i = \frac{x_i}{\sum_{i=1}^{N} \frac{x_i}{f(C_i^{\circ})}} \tag{5}$$

The IAS model described above was used in order to predict ternary solute adsorption data. The prediction of the binary solute adsorption data was performed via the LeVan–Vermeulen model [12]. This latter model is the IAS-based extension of the single-solute Langmuir model. Thus, the LeVan–Vermeulen model can be applied to each site of the bi-Langmuir model. Since the LeVan–Vermeulen model is explicit with respect to the solid-phase concentrations, the calculations of the competitive equilibria are faster with this model than with the IAS model defined by Eqs. (2)–(5). This fact is important when calculating overloaded band profiles.

3.2. Overloaded band profiles

For HPLC columns, which usually possess a high efficiency, the equilibrium–dispersive model is a good approximation to the solution of the system of mass balance equations that governs the separation process in the column [2]. In this case, the mass transfer in the column is assumed to be relatively fast, and the effects produced by the different resistances to mass transfer are lumped into an apparent Peclet number ($\mathrm{Pe}_{\mathrm{app}}$). Note that the equilibrium–dispersive model assumes that q_i and C_i are the equilibrium values related by the multicomponent adsorption isotherm.

For each component i in the column, the equilibrium–dispersive model is represented by the equation [13]:

$$\frac{\partial C_i}{\partial \theta} + \frac{\partial C_i}{\partial z} + \frac{(1-\epsilon_{\mathrm{T}})}{\epsilon_{\mathrm{T}}} \cdot \frac{\partial q_i}{\partial \theta} = \frac{1}{\mathrm{Pe}_{\mathrm{app}}} \cdot \frac{\partial^2 C_i}{\partial z^2} \tag{6}$$

where ϵ_{T} is the porosity of the packed bed and the nondimensional position (z) is defined as ($z = x/L$) where x is the actual position in the direction of the flow and L is the column length. The nondimensional time (θ) is defined by ($\tau = t/\tau$) where t is the actual time and τ is the residence or hold-up time as defined by $\tau = L/u$ where u is the interstitial velocity in the packed bed. In Eq. (6) the apparent Peclet number is defined by $\mathrm{Pe}_{\mathrm{app}} = 2N$, where N is the column plate number, an experimental parameter (note that $\mathrm{Pe}_{\mathrm{app}}$ is defined by reference to the apparent axial dispersion coefficient, not the molecular diffusivity). The value of N (see Table 1) is estimated from the chromatogram of an analytical injection (under linear conditions) of the solute of interest.

Suitable boundary conditions are needed to solve Eq. (6). The column is assumed to be empty of solutes at the beginning of the process [$C_i(z,0) = 0$], containing only the mobile phase in equilibrium with the stationary phase. The experimental injection profile at the column inlet is introduced in the calculations as the boundary condition. The set of Eq. (6) for different components is solved numerically using a finite-differences algorithm. In this study, we apply a forward–backward finite differences procedure based on the Godunov scheme [14]. The equilibrium–dispersive model has been applied successfully to the modeling of single solute and multisolute band profiles, provided there exist an accurate description of the associated adsorption equilibrium [2].

4. Discussion

The experimental system studied here is complex. As shown in Fig. 1 the structure of the compounds studied is more complex than the majority of the compounds used before in adsorption equilibrium determinations [2]. At pH 3.0 they are all protonated, thus exist in solution as cations. The nature of the mobile phase is also complex since it contains significant amounts of several inorganic ions (H^+, K^+, Cl^- and PO_4^{3-}). Thus, the similarity between the adsorption isotherms of DO and DI is striking, considering the marked differences between their structures. However, both possess a similar amino-alkyl chain which could be responsible for a significant part of the adsorbate–adsorbent interactions.

Table 1 and Fig. 2 show that doxepin is more retained than diltiazem at low concentrations, i.e., under linear conditions. It is clear, however, that the isotherm of diltiazem is above that of doxepin (Fig. 4). The reversal of the elution order of DO and DI when the concentration increases is a known phenomenon [15,16]. It takes place because the initial slope of the diltiazem isotherm (i.e., its Henry constant, $H = \Phi\kappa$) is lower (2.45) than that of doxepin (3.90) while the saturation capacity of diltiazem on the first site is higher (3.31 g/l) than that of doxepin (2.62 g/l). Thus the model properly accounts for the isotherm crossover at low concentrations. Note also that the maximum values of the products κC_i or λC_i are larger than 7 and between 0.3 and 0.5, respectively (maximum concentration, 10 g/l). This results in the accuracy of the determination of the first sets of coefficients being very accurate and the second only reasonably so [2].

The same reversal of the elution order of DO and DI also occurs when the pH of the mobile phase is increased to 6.0. Fig. 3 shows that diltiazem elutes last at pH 6.0 while doxepin is the most retained compound at pH 3.0 (see Fig. 2). Such changes in elution order as a result of modifications of the eluent pH is one of the key factors commonly employed for the optimization of analytical separations of organic cations [17].

Note in Fig. 4 that the dual site bi-Langmuir model provides an excellent correlation of all the single-solute adsorption data. As shown in Table 2, the site with the lower value of the saturation capacity has the larger value of the equilibrium constant. Thus, stronger adsorbate–adsorbent interactions take place in this site. The ratio between the saturation capacities of the two sites (Ψ/Φ) for the three drugs is in the range of 10–20 (see Table 2). In previous studies, this ratio was found as large as 60 [6].

A possible interpretation of this isotherm model would be to relate the two Langmuir contributions to the two main mechanisms [3] that govern the adsorption behavior of basic compounds such as DO, DI and BU on C_{18} phases: hydrophobic interactions (with either the bonded alkyl chains or the siloxane moieties) and ion-exchange with a subfraction of extremely acidic silanols. Several types of silanol are known to exist on the surface of silica gel, isolated, geminal and bonded vicinal species. The fraction of isolated, free silanols in the silica surface is believed to span a rather wide range of 1–50% [3,18]. Accordingly, the values of the ratio Ψ/Φ derived from the model and presented in Table 2 for the three drugs seem reasonable. The active, free silanols are those responsible for the strong interactions. Using temperature-programmed desorption of pyridine, for example, it was found that bonded silanols have a lower adsorption energy (ca. 60 kJ/mol) than isolated silanols (ca. 90 kJ/mol) [19]. On the other hand, the adsorption energy of neutral compounds on the alkyl chains from dilute solutions is usually of the order of 2.4 kcal/mol [19,20] (1 cal = 4.184 J). Note that the ratio of unreacted silanols to bonded alkyl chains on a typical octadecylsilica surface is of the order of unity. Accordingly, only a limited fraction of the unreacted silanols can be considered to belong to the strongly interacting sites. It is generally believed that these strongly acidic silanol sites are generated by metal traces buried in the silica matrix [3]. Because of the many uncertainties regarding the structure of the surface of C_{18} silicas, it is not possible to rationalize further the results of the isotherm determinations made in this work.

Note that the drugs studied here are able to sample the high energy sites despite the fact that the ionization of a large majority of the silanol groups is suppressed at pH 3.0 (the average bulk pK_a of the silanols is about 7.1–7.2) and only the most acidic

sites may remain dissociated and retain the ability of exchanging cations. Moreover, in this study we have used a rather concentrated buffer (0.1 *M*), a factor which should contribute further to reducing silanol ionization.

Another important issue to take into account is the fact that we employed acetonitrile rather than methanol as the organic modifier in the mobile phase. The peaks of basic compounds are usually more asymmetrical when using acetonitrile-based mobile phases at pH 7.0 [21]. Acetonitrile is unable to form hydrogen bonds with residual silanols, in contrast to methanol and tetrahydrofuran, so it cannot mask the silanols. It interacts mainly with the alkyl chains [22]. Thus, the presence of acetonitrile in the mobile phase should favor the interaction of the compounds studied with the active silanols. Recall that at pH 3.0 these compounds should be protonated and able to interact with the acidic silanols via the cation-exchange mechanism.

Another factor affecting the retention is the degree of protonation of the solutes. The pH of organic solvent–buffer solutions is always higher than the pH of the corresponding pure aqueous buffer. On the other hand, the pK_a of basic solutes is usually lower in acetonitrile–buffer solutions than in neat aqueous solutions. Several sets of published data summarize a consistent pattern of about -0.3 pK_a units per 10% addition of organic solvent to the buffer [3,23]. The higher the pK_a, the stronger the interactions of the solute with the strongly acidic silanols and the greater the degree of asymmetry of the bands. The pK_a values of buspirone, doxepin and diltiazem in aqueous, dilute solutions are between 8.0 and 9.0 [24]. In the buffer used, they are approximately 1 unit lower. Accordingly, these solutes will interact strongly with the silanol groups, especially at pH 3.0.

The single-component band profiles are reasonably well predicted by the model (Figs. 6–8). This agreement is in part a consequence of the high efficiency of the column for the studied solutes (see Table 1) since then the contribution of the finite column efficiency to the profile requires only a small correction that is well provided by the equilibrium–dispersive model [2]. It validates the isotherm data collected. There are some deviations at the top of the peaks, however, the calculated profiles being somewhat taller and sharper than the experimental ones.

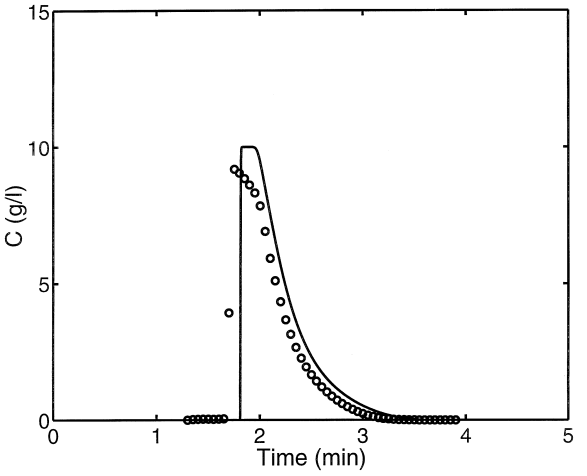

Fig. 6. Experimental (circles) and calculated (line) band profile of buspirone. Mobile phase is ACN–buffer (35:65); buffer is 0.1 *M* phosphate, pH 3.0, $T=25$°C, flow-rate is 1 ml/min, injected volume is 500 μl with a concentration of 10 g/l, UV detection at 345 nm.

The longer retention times of the calculated peaks is due to a slight overestimate of the retention factor at infinite dilution [$k=F(\Phi\kappa+\Psi\lambda)$]. It is to reduce the importance of such errors at low concentrations that the experimental data fitted to the isotherm model are weighed so as to minimize $\Sigma_i(q_{i,\,ex}-q_{i,\,th})^2/q_{i,\,th}^2$ in

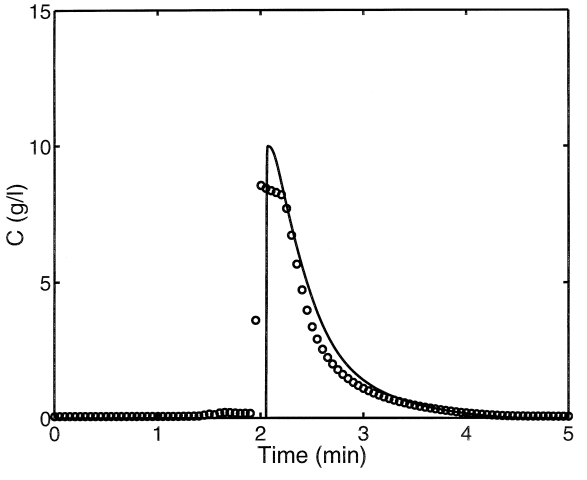

Fig. 7. Experimental (circles) and calculated (line) band profile of doxepin. Mobile phase is ACN–buffer (35:65); buffer is 0.1 *M* phosphate, pH 3.0, $T=25$°C, flow-rate is 1 ml/min, injected volume is 500 μl with a concentration of 10 g/l, UV detection at 325 nm.

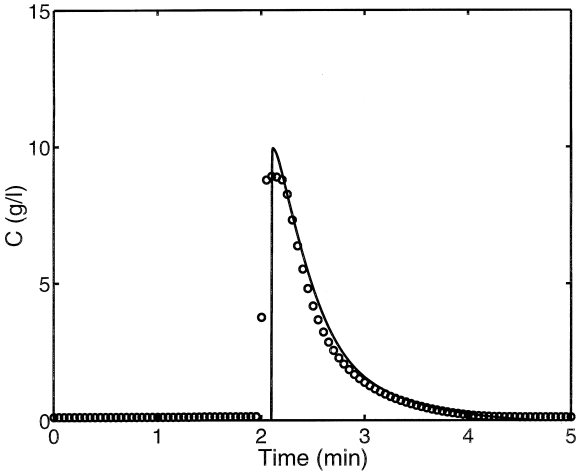

Fig. 8. Experimental (circles) and calculated (line) band profile of diltiazem. Mobile phase is ACN–buffer (35:65); buffer is 0.1 *M* phosphate, pH 3.0, $T=25$°C, flow-rate is 1 ml/min, injected volume is 500 μl with a concentration of 10 g/l, UV detection at 300 nm.

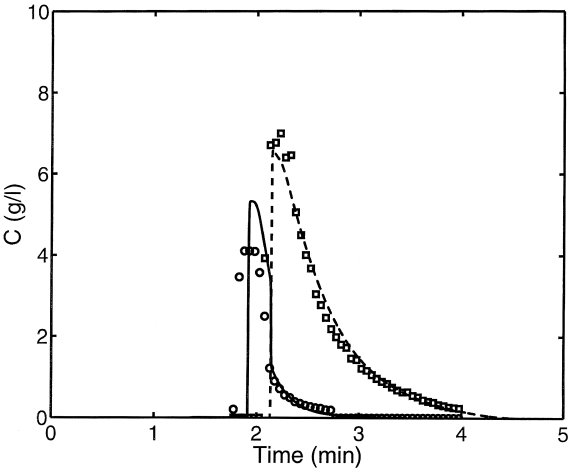

Fig. 9. Experimental (symbols) and calculated (lines) band profiles of buspirone (circles and solid line) and diltiazem (squares and dashed line). Mobile phase is ACN–buffer (35:65); buffer is 0.1 *M* phosphate, pH 3.0, $T=25$ °C, flow-rate is 1 ml/min, injected volume is 500 μl with a total solute concentration of 10 g/l, the mass ratio of BU:DI=1:3 (w/w), UV detection at 300 nm.

the regression [2]. Note also that the tailing of the BU band presented in Fig. 6 is less pronounced than the tailing of the DO and DI bands presented in Figs. 7 and 8, respectively. Most of this tailing is well accounted for by the bi-Langmuir isotherm model. It is possible that the steric hindrance around the nitrogen atoms in BU (located in the rings) is greater than in the other two compounds, the nitrogen atom of which is located at the end of a lateral chain. The long peak tailing observed in Figs. 7 and 8 was often reported in the chromatography of basic compounds [3]. It is considered to be a result of the presence of a subfraction of the surface silanols with enhanced acidity which interact strongly with the protonated organic bases.

Multisolute profiles corresponding to samples of the three possible binaries and of the ternary mixture of the three compounds are also well predicted, as shown in Figs. 9–12. The good agreement between calculated and experimental profiles constitutes an indirect confirmation that the competitive equilibria of the three compounds follow the IAS model. Note in Fig. 11 that the shocks of DO and DI coincide, a result of the closeness of the isotherms of these two components (see Fig. 4). Finally, in Fig. 13, a single-solute system peak is presented for the injection of BU in a stream containing DI. In this case also, the model accounts reasonably well for the experimental profile of the elution band of BU. The differences observed in the retention times of the shock layers are due to errors made in the estimate of the

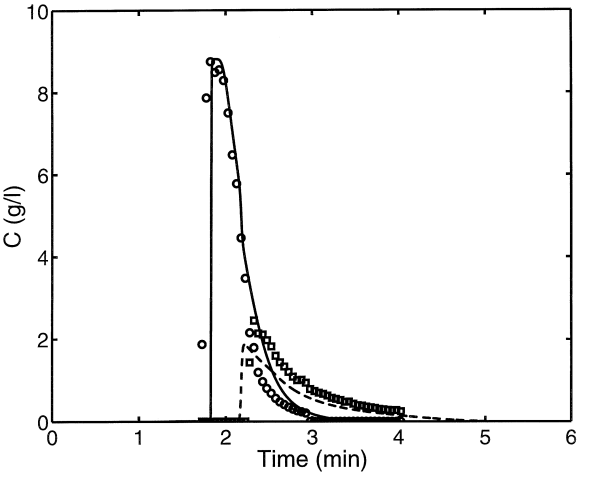

Fig. 10. Experimental (symbols) and calculated (lines) band profiles of buspirone (circles and solid line) and doxepin (squares and dashed line). Mobile phase is ACN–buffer (35:65); buffer is 0.1 *M* phosphate, pH 3.0, $T=25$°C, flow-rate is 1 ml/min, injected volume is 500 μl with a total solute concentration of 10 g/l, the mass ratio of BU:DO=3:1 (w/w), UV detection at 300 nm.

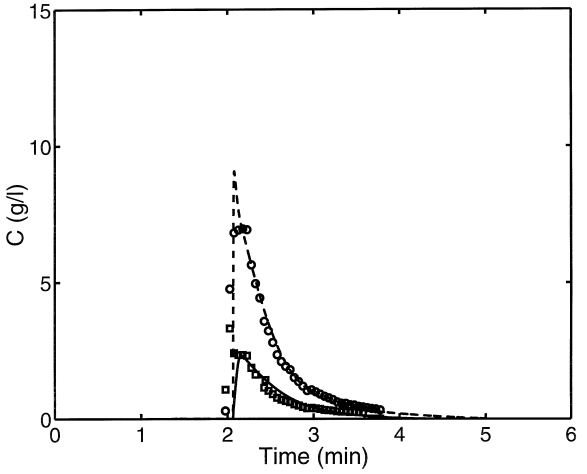

Fig. 11. Experimental (symbols) and calculated (lines) band profiles of diltiazem (squares and solid line) and doxepin (circles and dashed line). Mobile phase is ACN–buffer (35:65); buffer is 0.1 *M* phosphate, pH 3.0, $T=25$°C, flow-rate is 1 ml/min, injected volume is 500 μl with a total solute concentration of 10 g/l, the mass ratio of DI:DO=1:3 (w/w), UV detection at 300 nm.

retention factors at infinite dilution (see paragraph above). The differences in band height arise from errors in the estimate of the saturation capacities.

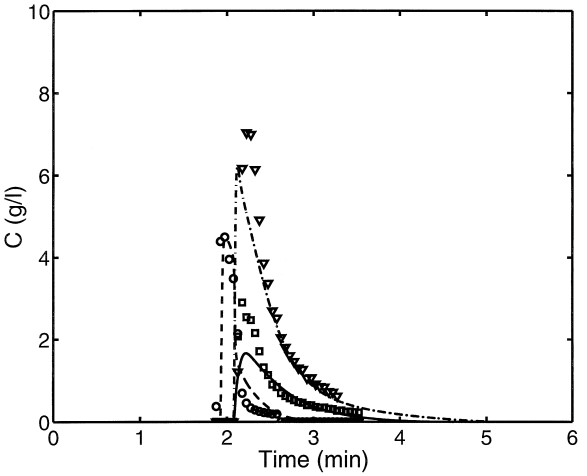

Fig. 12. Experimental (symbols) and calculated (lines) band profiles of buspirone (circles and dashed line), diltiazem (squares and solid line) and doxepin (triangles and dashed-dotted line). Mobile phase is ACN–buffer (35:65); buffer is 0.1 *M* phosphate, pH 3.0, $T=25$ °C, flow-rate is 1 ml/min, injected volume is 500 μl with a total solute concentration of 10 g/l, the mass ratio of BU:DI:DO=1:1:3 (w/w), UV detection at 300 nm.

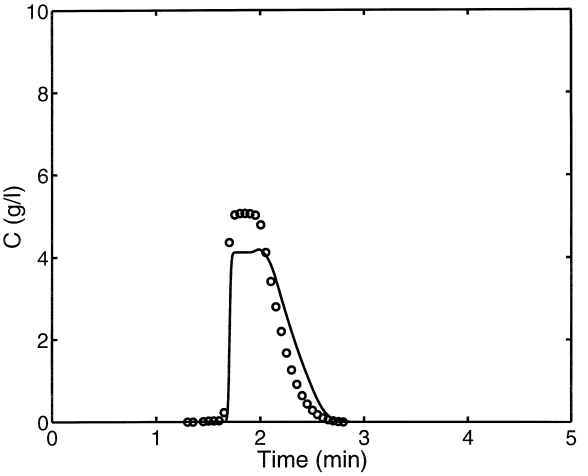

Fig. 13. Experimental (circles) and calculated (solid line) system peak of buspirone. The mobile phase contains 4 g/l of diltiazem in ACN–buffer (35:65, v/v). The buffer is 0.1 *M* phosphate, pH 3.0, $T=25$°C, flow-rate is 1 ml/min, injected volume is 500 μl with a buspirone concentration of 5 g/l, UV detection at 345 nm.

More complex models of competitive equilibrium isotherms could, in principle, be used. However, the model used in this work is already based on four-parameter isotherm equations (bi-Langmuir model, Eq. (1)). The experimental data obtained are rarely precise enough and collected in a wide enough range of concentrations (e.g., for solubility reasons) to warrant the use of more complex single-component isotherm models, which would require the determination of more parameters. The parameters of more complex competitive models based on four-parameter single-component isotherms cannot be determined if competitive isotherm data cannot be measured because the additional terms are function of C_iC_j and do not contribute to single-component equilibrium data.

5. Conclusion

The single-solute phase equilibria in a complex experimental system of three ionized compounds adsorbing on a C_{18} column from a buffered mobile phase can be well described using the bi-Langmuir model. This result suggests that, according to the model, adsorption takes place on two different types of sites and that there are two different retention

mechanisms. Hydrophobic interactions take place on low-energy sites (alkyl chains) and ion-exchange interactions on high energy sites (highly acidic silanols). These results confirm previous findings regarding reversed-phase liquid chromatographic separations of basic solutes [3]. Further work is needed, however, to ascertain this conclusion which, at this stage, can only be tentative.

Competitive adsorption equilibria were predicted using the IAS model in order to calculate multisolute band profiles via the equilibrium–dispersive model. As a result, a good representation of the overloaded band profiles and of the system peaks measured in the system under consideration was obtained. This fact is an indirect confirmation that the multisolute adsorption data is well predicted from the single-solute data via the IAS formalism. Since the system is clearly nonideal, this latter fact could be a result of rather constant activity coefficients in both phases at equilibrium, as discussed elsewhere [19].

Finally, this work demonstrates that it is not exceedingly difficult nor time-consuming to acquire the experimental data required to avail oneself of the fundamental results of nonlinear chromatography. Having modeled the single-component equilibrium data acquired by frontal analysis for each compound involved, one can use an IAS-based extension of these models to derive simply a competitive isotherm model for the mixture investigated. If the single-component data are accurately measured good agreement should be expected between band profiles measured and calculated. Then, it is easy to calculate reasonable estimates of the optimum conditions under which to run preparative chromatography by overloaded elution of simulated moving bed separation. Minor adjustments of these conditions must be made but the final tuning of the process should be easier, faster, and much less expensive than the conventional trial-and-error approach.

Acknowledgements

This work was supported in part by Grant CHE-97-01680 of the National Science Foundation and by the cooperative agreement between the University of Tennessee and the Oak Ridge National Laboratory. The research stay of A.C. was made possible by NATO grant OUTR.LG 971480. We acknowledge the support of Maureen S. Smith in solving our computational problems and fruitful discussions of this work with Zoubair El Fallah and Marianna Kele.

References

[1] S.C. Stinson, Chem. Eng. News 73 (1995) 44.
[2] G. Guiochon, S.G. Shirazi, A.M. Katti, Fundamentals of Preparative and Nonlinear Chromatography, Academic Press, Boston, MA, 1994.
[3] J. Nawrocki, J. Chromatogr. A 779 (1997) 29.
[4] T. Fornstedt, P. Sajonz, G. Guiochon, Chirality 10 (1998) 375.
[5] T. Fornstedt, G. Gotmar, M. Andersson, G. Guiochon, J. Am. Chem. Soc. 121 (1999) 1164.
[6] J.E. Eble, R.L. Grob, P.E. Antle, L.R. Snyder, J. Chromatogr. 384 (1987) 45.
[7] 11th Edition, The Merck Index, Merck, Rahway, NJ, 1989, Compounds 1493, 3188 and 3425.
[8] J.J. Jacobson, J. Frenz, Cs. Horvath, J. Chromatogr. 316 (1984) 53.
[9] NAG, The Numerical Algorithms Group, The NAG Fortran Library Manual, Mark 16, NAG, Downers Grove, 1993.
[10] A.L. Myers, J.M. Prausnitz, AIChE J. 11 (1965) 121.
[11] C.J. Radke, J.M. Prausnitz, AIChE J. 18 (1972) 761.
[12] M.D. LeVan, T. Vermeulen, J. Phys. Chem. 85 (1981) 3247.
[13] H. Rhee, B.F. Bodin, N.R. Amundson, Chem. Eng. Sci. 26 (1971) 1571.
[14] P. Rouchon, P. Valentin, M. Schonauer, G. Guiochon, Sep. Sci. Technol. 22 (1987) 1793.
[15] F.D. Antia, Cs. Horvath, J. Chromatogr. 556 (1991) 119.
[16] S. Golshan-Shirazi, J.-X. Huang, G. Guiochon, Anal. Chem. 63 (1991) 1147.
[17] L.R. Snyder, J.J. Kirkland, J.L. Glajch, Practical HPLC Method Development,, Wiley, New York, 1997.
[18] I. Gillis-D'Hamers, I. Cornelissens, K.C. Vrancken, P.V.D. Voort, E.F. Vansant, J. Chem. Soc., Faraday Trans. 88 (1992) 723.
[19] I. Quinones, J.C. Ford, G. Guiochon, Chem. Eng. Sci. (1999) in press.
[20] K. Miyabe, M. Suzuki, AIChE J. 38 (1992) 901.
[21] D.V. McCalley, J. Chromatogr. A 769 (1997) 169.
[22] Y.V. Kazakevich, H.M. McNair, J. Chromatogr. Sci. 33 (1995) 321.
[23] E. Bosch, S. Espinosa, M. Roses, J. Chromatogr. A 824 (1998) 137.
[24] CompuDrug Chemistry, pKalc Expert System, CompuDrug Chemistry, Budapest, 1992.